Environmental Geochemistry and Health

CHARACTERIZATION OF THE BIOAEROSOL IN A NATURAL THERMAL CAVE AND ASSESSMENT OF THE RISK OF TRANSMISSION OF SARS-COV-2 VIRUS

--Manuscript Draft--

Manuscript Number:	
Full Title:	CHARACTERIZATION OF THE BIOAEROSOL IN A NATURAL THERMAL CAVE AND ASSESSMENT OF THE RISK OF TRANSMISSION OF SARS-COV-2 VIRUS
Article Type:	Original Research
Keywords:	thermal cave; bioaerosol; risk of transmission; SARS-CoV-2 virus; viral droplets; atypical indoor environments
Corresponding Author:	Eleonora Carota, Ph.D. University of Tuscia: Universita degli Studi della Tuscia Viterbo, Viterbo ITALY
Corresponding Author Secondary Information:	
Corresponding Author's Institution:	University of Tuscia: Universita degli Studi della Tuscia
Corresponding Author's Secondary Institution:	
First Author:	Mauro Scungio, Ph.D.
First Author Secondary Information:	
Order of Authors:	Mauro Scungio, Ph.D.
	Silvia Crognale, Ph.D.
	Davide Lelli, Bachelor
	Eleonora Carota, Ph.D.
	Giuseppe Calabrò
Order of Authors Secondary Information:	
Funding Information:	University of Tuscia (“Action for research activities related to COVID-19emergency” Rector note n°5445, 05-05-2020,) — Not applicable
	Terme dei Papi (Viterbo, Italy) (“Characterization of Bioaerosol in the Thermal Cave of Terme dei Papi and effect of environmental conditions in the decay and transmission of biological agents”) — Not applicable

Abstract:

Thermal caves represent an environment characterized by unique chemical-physical properties, often used by customers for treatment and care of musculoskeletal, respiratory and skin diseases.

However, these environments are poorly characterized for their physical and microbiological characteristics; furthermore, the recent pandemic caused by COVID-19 has highlighted the need to investigate the potential transmission scenario of SARS-CoV-2 virus in indoor environments where an in-depth analysis of the aerosol concentrations and dimensional distributions are essential in order to monitor the spread of the virus.

This research work was carried out inside a natural cave located in Viterbo (Terme dei Papi, Italy) where a waterfall of sulfur-sulfate-bicarbonate-alkaline earth mineral thermal water creates a warm-humid environment with 100% humidity and 48°C temperature. A characterization of the aerosol and bioaerosol was carried out to estimate the personal exposure to aerosol concentrations, as well as particle size distributions and to give an indication of the native microbial load.

The data obtained showed a predominance of particles with a diameter greater than 8

	µm, associated with a low ability of penetration in the human respiratory system. A low microbial load was also observed, with a prevalence of non-cultivable strains generated by the aerosolization of the thermal waters. Finally, the estimation of SARS-CoV-2 infection risk by means of mathematical modelling revealed a low risk of transmission, with a decisive effect given by the mechanical ventilation system, which, together with the adoption of social distancing measures makes the risk of infection extremely low.
Suggested Reviewers:	Federica Valeriani, Ph.D. Researcher, University of Rome 'Foro Italico': Universita degli Studi di Roma 'Foro Italico' federica.valeriani@uniroma4.it Expert in Swimming Pools and Thermal facilities safety and prevention
	Satbir Singh, Ph.D. Associate Professor, Carnegie Mellon University, Pittsburgh, PA, USA satbirs@andrew.cmu.edu Expert in aerosol physical characterization
	Pasquale Avino, Ph.D. Researcher, Università del Molise (Italy) avino@unimol.it Expert in air quality
	Maarten G.A. Keuten, Ph.D. Researcher, Delft University of Technology: Technische Universiteit Delft m.g.a.keuten@tudelft.nl Expert on anthropogenic pollutant release in swimming pools
	Athena Th Mavridou, Ph.D. Professor, University of West Attica: Panepistemio Dytikes Attikes amavridou@uniwa.gr Member of the International Water Association (IWA) Health -Related Water Microbiology Group (HRWM), expert on pool and SPA regulations and on pathogens

Title: CHARACTERIZATION OF THE BIOAEROSOL IN A NATURAL THERMAL CAVE AND ASSESSMENT OF THE RISK OF TRANSMISSION OF SARS-COV-2 VIRUS

Mauro Scungio[1], Silvia Crognale[2], Davide Lelli[2] Eleonora Carota[2], Giuseppe Calabrò[1]*

[1] Department of Economics, Engineering, Society and Business Organization (DEIM), University of Tuscia, Via del Paradiso 47, Viterbo, Italy

[2] Department for Innovation in Biological, Agro-food and Forest Systems (DIBAF), University of Tuscia, Via San Camillo de Lellis, Viterbo, Italy

(*) Correspondence should be addressed to:

Eleonora Carota

e-mail: carota@unitus.it

ORCID iDs of authors

Eleonora Carota: 0000-0002-9116-7310

Mauro Scungio: 0000-0001-6375-0464

Silvia Crognale: 0000-0001-5249-70533

Giuseppe Calabrò: 0000-0002-7277-1125

Abstract

Thermal caves represent an environment characterized by unique chemical-physical properties, often used by customers for treatment and care of musculoskeletal, respiratory and skin diseases.

However, these environments are poorly characterized for their physical and microbiological characteristics; furthermore, the recent pandemic caused by COVID-19 has highlighted the need to investigate the potential transmission scenario of *SARS-CoV-2* virus in indoor environments where an in-depth analysis of the aerosol concentrations and dimensional distributions are essential in order to monitor the spread of the virus.

This research work was carried out inside a natural cave located in Viterbo (Terme dei Papi, Italy) where a waterfall of sulfur-sulfate-bicarbonate-alkaline earth mineral thermal water creates a warm-humid environment with 100% humidity and 48°C temperature. A characterization of the aerosol and bioaerosol was carried out to estimate the personal exposure to aerosol concentrations, as well as particle size distributions and to give an indication of the native microbial load.

The data obtained showed a predominance of particles with a diameter greater than 8 µm, associated with a low ability of penetration in the human respiratory system. A low microbial load was also observed, with a prevalence of non-cultivable strains generated by the aerosolization of the thermal waters.

Finally, the estimation of SARS-CoV-2 infection risk by means of mathematical modelling revealed a low risk of transmission, with a decisive effect given by the mechanical ventilation system, which, together with the adoption of social distancing measures makes the risk of infection extremely low.

Key words: thermal cave; bioaerosol; risk of transmission; SARS-CoV-2 virus; viral droplets; atypical indoor environments

Introduction

Thermal facilities, such as caves, swimming pools and SPAs, represent an environment characterized by unique chemical-physical properties, such as the high concentration of mineral salts and dissolved gases, peculiar temperatures and pH. Depending on the content of specific elements in the thermal waters, such as bicarbonates, calcium, sulphur, sulphates, chlorides, radon, iron, magnesium, potassium, lithium, arsenic and silica, different therapeutic effects for musculoskeletal, respiratory and skin diseases can be observed (Altman 2000).

However, the recent pandemic caused by COVID-19 has imposed the need to investigate the potential transmission scenario of *SARS-CoV-2* virus also in such atypical and poorly studied indoor environments, where an in-depth analysis of the aerosol concentrations and dimensional distributions are essential in order to monitor the spread of the virus. While some studies and models have been proposed to estimate the airborne risk of transmission in public environments such as hospitals (Chia et al. 2020; Guo et al. 2020; Liu et al. 2020) or restaurants (Buonanno et al. 2020a Li et al. 2020), characterized by mild climatic conditions in terms of temperature and relative humidity, thermal environments have been poorly investigated; furthermore, the specific properties of these environments prevent their treatment and the application of conventional disinfection procedures in order to preserve their health benefits during balneotherapy or other treatments (Margarucci et al., 2019).

The main route of transmission of the SARS-CoV-2 virus to humans occurs predominantly via the respiratory route, by means of both small and large droplets (Morawska et al., 2020; WHO, 2020). The risk of transmission is dependent on different factors, such droplet properties, indoor airflow and virus characteristics. Droplet size influences both the deposition mechanisms and the extent of penetration in the human respiratory systems. Small droplets (1-5 µm) can remain suspended in the air for many hours and penetrate up to the alveoli, while larger droplets have a high sedimentation rate and deposit in the upper respiratory tract (Ghosh et al. 2015; Thomas et al. 2008). Moreover, being droplets constituted mostly of water associated with an aerosol-size nucleus, the evaporation kinetics, influenced by relative humidity and air temperature, affect their lifetime and deposition (Kohanski et al. 2020).

In addition to the chemical-physical characteristics of the aerosol particles, ventilation systems and convection currents play a critical role in indoor environments: if appropriate, they can promote the removal of exhaled virus-laden air, thus lowering the airborne viral concentration; in case of inefficient or obstructed airflow, they can disperse the aerosol over a large area, with the potential to increase the risk of transmission to other occupants (Morawska et al. 2020).

The abiotic matter of the aerosol is generally associated with compounds of biological origin, including all pathogenic or non-pathogenic, live or dead fungi and bacteria, viruses, spores, pollens and microbial secondary metabolites, which give origin to the so-called bioaerosol (Ghosh et al. 2015). Different studies concerning indoor air quality have found that between 5 to 34% of indoor air pollution is caused by biological compounds. The characterization of bioaerosol components is the subject of growing interest in the scientific community, especially for the effects that these components have on human health: infections, asthma, allergies and other diseases of the respiratory tract (Srikanth et al., 2008).

The risks are influenced not only by the ability of the aerosol to penetrate the respiratory system, but also by its composition and biological activity. Bioaerosol composition is mainly dependent on the physical characteristics of the droplets or particles (e.g. size, density, and shape) and on environmental factors such as relative humidity, temperature, light intensity, moisture content of building material (Ghosh et al. 2015). Therefore, the microbiological air quality is another important parameter to take into account in a risk assessment plan.

For risk management in the initial phase of reopening of the thermal structures, some protocols and self-control plans have been developed but the development of new scientific evidence on this is desirable.

This research work was carried out inside a natural thermal cave located in Italy (Terme dei Papi, Viterbo) where a waterfall of sulfur-sulfate-bicarbonate-alkaline earth mineral thermal water creates a warm-humid environment with 100% humidity and 48°C temperature. A characterization of the aerosol and bioaerosol was carried out with the aim of estimating personal exposure to aerosol concentrations in terms of number, surface area and mass, as well as particle size distributions, to evaluate the distribution inside the cave of these concentrations and to give an indication of the levels of the native microbial load. The final purpose was the identification of specific thresholds and alert values to support the development of a Risk Assessment Plan in thermal caves.

Materials and methods

Aerosol characterization

Bioaerosol active sampling

Air samples were collected by impaction with a single-stage air sampler Microflow α (AQUARIA srl, Italy), holding 380 jets with a diameter of 1 mm. The sampler was placed in a central position of the cave at 1-meter height. The impaction flow rate was set at 120 L/min and the air stream was directed on 90 mm diameter agar Petri dishes containing different growth media, mainly Lysogeny Broth Agar (LBA) (10 g/l NaCl (Sigma-Aldrich, USA), 5 g/l yeast extract (Merck, Germany), 15 g/l agar (Difco, Michigan) and Plate Count Agar (PCA) (Difco, Michigan), or on cellulose nitrate filters with a pore size of 0.45 µm (Sartorius, Germany). Different sampling volumes, between 250 and 1000 L, were collected in duplicate. The resulting Petri dishes were incubated at 25°C and 50°C for 12 hours and the number of bacterial or fungal colonies was expressed as colony-forming units per cubic meter (CFU/m^3). Filters were stored at -20 °C in sterile tubes until genomic DNA extraction.

Quantitative PCR analysis for microbial load determination

Total DNA was extracted from the bioaerosol collected on filters by using the DNeasy PowerWater kit (QIAGEN, Hilden, Germany) as described in the manufacturer's instructions.

Fungal and bacterial abundances were determined by q-PCR of 18S rRNA and 16S rRNA genes, respectively, on a LightCycler R 480 System (Roche Applied Science, USA). 18S rDNA sequences were amplified using the primer pair FR1F (5′-AICCATTCAATCGGTAIT-3′) and FF 390R (5-′CGATAACGAACGAGACCT-3′), while 16S rDNA sequences using the primer pair 331F (5′-TCCTACGGGAGGCAGCAGT-3′) and 797R, (5′-GGACTACCAGGGTATCTAATCCTGTT-3′). The protocol and optimized conditions described in Crognale et al. (2019) were applied. Melting curve analysis of the PCR products was performed to confirm that the fluorescence signals derived from specific PCR products. Fungal and bacterial concentrations were calculated based on a standard curve obtained using triplicate 10-fold serial dilutions ($10^2 – 10^{10}$ 18S or 16S copy number) of known concentration of plasmid pGem T-easy cloning vector containing the target gene as the insert.

Bioaerosol passive sampling

90 mm Petri dishes containing LBA or PCA medium were exposed to air for 2 hours in a central position of the thermal cave, at 1-meter height and subsequently incubated at 25°C and 50°C for 12 hours. Counts of bacterial fungal colonies were expressed as colony-forming units per square meter per hour of exposure (CFU/(m^2·h)).

Aerosol physical characteristics measurements

The physical characteristics of the aerosol were measured by means of an optical spectrometer (OPS model 3330, TSI, Minnesota, USA). The OPS was calibrated by means of tests made in the European Accredited Laboratory of Industrial Measurements (LAMI) at the University of Cassino and Southern Lazio (Italy).

The samplings were repeated in two different days and in two distinct moments: at the morning before the first entrance to the cave and at the evening after the last entrance. Each measurement represented the average of several samplings lasting 100 seconds and was related to a number, surface area and mass concentration and size distributions of particles per unit volume of sampled air.

Starting from the size distributions of the aerosol measured in the cave and using appropriate deposition curves (ICRP, 1994), the lung-deposited fraction of inhaled particles was calculated.

SARS-CoV-2 transmission risk evaluation

To evaluate the airborne transmission risk of SARS-CoV-2 inside the cave, a model recently proposed by Buonanno et al. (2020a/b) was adopted. The model is able to quantify the probability of infection due to exposure in a microenvironment in presence of a SARS-CoV-2 infected subject, by means of a four step approach: (i) evaluation of the quanta emission rate (quanta is defined as the dose of airborne droplet nuclei required to cause infection in 63% of susceptible persons (Buonanno et al 2020a); (ii) evaluation of the exposure to quanta concentration in the microenvironment; (iii) evaluation of the dose of quanta received by an exposed susceptible subject; and (iv) estimation of the probability of infection on the basis of a dose–response model. These four steps are briefly described in hereafter, referring to the original papers for more details (Buonanno et al. 2020 a/b).

The quanta emission rate (ER_q, quanta h^{-1}) is evaluated as (first step):

$$ER_q = c_v \cdot c_i \cdot IR \cdot V_d = c_v \cdot \frac{1}{C_{RNA} \cdot C_{PFU}} \cdot IR \cdot V_d$$

where c_v (RNA copies mL^{-1}) is the viral load in the exhaled droplets, c_i (quanta RNA copies $^{-1}$) is a conversion factor, IR is the inhalation rate (m^3 h^{-1}), and V_d is the exhaled droplet volume concentration (mL m^{-3}), which depends on the repiratory activity.

The quanta concentration at time t to which a susceptible subject is exposed in an indoor environment is based on a mass balance and can be evaluated as (second step):

$$n(t, ER_q) = n_0 \cdot e^{-IVRR \cdot t} + \frac{ER_q \cdot I}{IVRR \cdot V} \cdot (1 - e^{-IVRR \cdot t})$$

where IVRR (h^{-1}) represents the infectious virus removal rate, n_0 represents the initial quanta concentration, I is the number of infectious subjects, V is the volume of the indoor environment, and ER_q is the quanta emission rate for the virus under investigation. IVRR depends on three mechanisms: air exchange rate via ventilation, particle deposition on surfaces and viral inactivation. There are three important hypotheses on the quanta concentration calculation: the infectious virus removal rate is constant, the latent period of the disease is longer than the time scale of the model, and the droplets are instantaneously and evenly distributed in the indoor environment.

The dose of quanta received by an exposed susceptible subject to the quanta concentration, for a certain time interval (T), is evaluated as (third step):

$$D_q(ER_q) = IR\int_0^T n(t)dt$$

The probability of infection is calculated by an exponential dose-response model as (fourth step):

$$P_I = 1 - e^{-D_q}$$

Finally, the individual infection risk (R) of an exposed subject is calculated as the product of the probability of infection and the probability of occurrence of the specific ER_q value, while the basic reproduction number (R_0) is evaluated by multiplying the individual infection risk by the number of exposed susceptible individuals (Buonanno et al. 2020a).

Model parameters and hypothesized scenarios for the risk of infection transmission inside the cave

The parameters set as input data of the model, described in detail below, are: volume of the cave (V); total infectious viral removal rate (IVRR), which is the sum of the number of air exchanges per hour (AER), the deposition rate of particles on the surfaces (k) and rate of viral inactivation (λ); initial concentration of quanta (n_0); total time of occupation of the cave (t).

The volume of the cave was calculated directly from measurements carried out on site and is equal to 34 m^3 while the number of hourly changes of air was obtained from the technical specifications of the ventilation system installed (260 m^3 h^{-1}) plus 0.2 h^{-1} to take into account the infiltrations deriving from the partial opening of the skylight, for a total of AER equal to 7.78 h^{-1}. The deposition rate of the particles (k) was set equal to 0.24 h^{-1} as proposed by Buonanno et al. (2020a) which calculated the deposition rate as the ratio between the sedimentation rate of particles whose diameter is greater than 1 µm (approximately 1.0×10^{-4} m s^{-1} as measured by Chatoutsidou and Lazaridis (2019) and the height of the emission source (1.5 m). The viral inactivation rate (λ) was set equal to 0.63 h^{-1} based on the value of the SARS-CoV-2 half-life (1.1 hours) detected by van Doremalen et al. (2020) as follows:

$$\lambda\ (h^{-1}) = \frac{0.693}{t_{1/2}}$$

Finally, the initial quanta concentration (n_0) and the total occupation time of the cave (t) were set equal to zero and 8 hours, respectively. All the parameters are shown in detail in Table 1.

As regards the hypothesized scenarios, these have been implemented by setting the following parameters: time of entry and exit from the cave and the emission rate of quanta of infectious subjects (ER_q); time of entry and exit from the cave and inhalation rate (IR) of the susceptible subject. In particular, we hypothesized four scenarios: the first (S1) involves the consecutive entry into the cave of two infectious subjects, for a residence time of 15 minutes for each, and subsequent entry into the cave of the susceptible subject, with a residence time of the latter equal to 15 minutes; the second (S2) involves the entry and stay of two infectious subjects and a susceptible subject simultaneously for 15 minutes. In the first scenario (S1) all the occupants were considered to be at rest (seated) and characterized only by respiratory activity, while in the second (S2) the occupants are considered to be standing and talking to each other. Both S1 and S2 scenarios have been implemented considering the ventilation system in operation and semi-opened skylight (AER = 7.78 h^{-1}). Starting for S1 and S2, two additional scenarios were considered: S3 (same of S1 without the ventilation system active) and S4 (same of S2 without the ventilation system active). For S3 and S4, however, an AER value of 0.2 h^{-1} was imposed to take into account infiltrations through the doors. Details of the simulated scenarios are reported in Table 2.

Results

Bioaerosol characterization inside the thermal cave

Microbiological sampling of the air is based on the capture of the corpuscular component of the aerosol, containing the biological fraction that is intended to be evaluated. The collection of airborne particles can be obtained through the use of passive sampling techniques, based on the inertial deposition of the microbiological fraction on a given surface, or through active sampling, based on the active aspiration of air with a controlled flow rate and volume of aspiration.

In Table 3 the microbial load values deriving from active and passive sampling techniques and from independent method are shown. The colonies collected in both active and passive samples were mostly bacterial (data not shown), although some few fungal colonies were observed. This result is also confirmed by molecular data where the value of 18S copy number/m^3, associated to fungal species, is two orders of magnitude lower than that of 16S, related to bacteria.

Values of microbial load deriving from passive sampling showed a predominance of termophilic species, part of which was presumably able to grow even in mesophilic conditions. In active sampling, instead, the mesophilic and thermophilic microbial load values are comparable, probably due to a different fraction of collected microorganisms,

Physical characteristics of the aerosol inside the thermal cave

In this section the results of the measurements made inside the thermal cave are reported. The data are shown as size distributions (Fig. 1) and average concentrations (Table 4) in terms of number (N), surface area (SA) and mass (M) of particles. Since no significant changes in the aerosol characteristics were observed between the two days of measurements, and between morning and evening for each day, the data are shown as average values with the relative standard deviation among all the measurements carried out.

Starting from the size distributions of the aerosol measured in the cave and using appropriate deposition curves obtained from the ICRP data for the particle size range considered in this study (0.3 – 10 µm), it is possible to estimate the fraction of particles that deposit within the respiratory system. The deposition curves are showed in Fig. 2 while a summary of the concentration in terms of number, surface area and mass of particles deposited in the respiratory system is reported in Table 5.

Risk of infection transmission inside the thermal cave

On the basis of the methodology described in the "Materials and methods" section, the risk of SARS-CoV-2 transmission inside the cave is in hereafter reported for the susceptible occupant (relative to his residence time) and for the susceptible persons (i.e., relative to the total time of occupation). The results of the simulations are reported in the following tables as follows: (i) exposure time (t_{exp}) which is the exit time minus the entry time in minutes for the susceptible subject and the total time of occupation for continuous occupation; (ii) individual infection risk (R) which represents the percentage probability of individual infection for the exposure to the quanta concentration profile integrated over the exposure time; (iii) exposure time for 1% and 0.1% risk ($t_{exp,1}$ and $t_{exp,0.1}$) which is the exposure time in minutes associated with a 1% and 0.1% probability of infection in order to consider different cohorts of individuals (younger-healthier individuals and weaker-older people, respectively); (iv) maximum occupation of the cave for R_0 <1 ($O_{max,R<1}$) which represents the maximum number of occupants theoretically allowed in the cave for the exposure time and the quanta concentration profile of the designated scenario in order to keep the base reproduction number (R_0) below 1.

In Table 6 the symbol “greater than” means that the susceptible subject or the continuous occupation does not exceed the 0.1% or 1% risk threshold.
Fig. 3 shows the variation over the whole simulation time of the model results for each scenario hypothesized: quanta concentration in the cave; individual risk of infection for the susceptible subject; individual risk of infection for a subject who continuously occupies the cave for the entire simulated time; maximum theoretical occupancy of the cave to maintain R_0<1 (for a cohort that enters in the cave at the zero instant, continuous occupation).

Discussions

Bioaerosol characterization inside the thermal cave

As shown in Table 3, the active and passive sampling methods yield results that are not directly comparable, as they have different purposes: passive sampling is mainly used to measure the settling speed of particles on surfaces (CFU/(m^2·h)), while active sampling is used to measure the average concentration of airborne microorganisms (CFU/m^3) (Cabral, 2010). Nowadays, there are no worldwide accepted regulations for microbial exposure assessment in different environments with the exception of those elaborated for the control of the working environment summarized in four European standards: EN 13098:2000, EN 14031:2003, EN 14042:2003 and EN 14583:2004. However, these standards refer only to the methodology to be followed but do not specify threshold values for microbial load. The only reference to evaluate the contamination levels is a document from the European Collaborative Action (EUR 14988) reporting the indicative levels of microbial air contamination by means of active sampling, the exceeding of which does not automatically imply the establishment of dangerous or unhealthy conditions.
Referring to these guidelines a microbial load <100 CFU/m^3, as those observed in the thermal cave under study, is considered a very low level of contamination. Given the particular conditions of the thermal environment, in addition to the reference incubation temperature for mesophilic microorganisms of 25 °C, the plates were also incubated at 50°C to evaluate also the thermophilic microbial fraction. Even in the latter case, the microbial load values were fully within a very low level of contamination.
Regarding the passive sampling technique, although its provides an idea of the amount of biological agents that undergo sedimentation per hour, it is not possible to establish any thresholds since it is not a quantitative method, it does not allow to correlate the number of microorganisms at a known volume of air and has a very low sensitivity. However, it can be considered as a qualitative parameter to describe the fate of particles in bioaerosol. In this study, the passive sampling could collect a high number of microorganisms probably due to the fact that the bioaerosol was mainly composed of large-size particles (≥10 um) characterized by a high sedimentation rate (Cabral 2010).
In addition to culture-dependent traditional microbiological methods, a further quantification of the airborne microbial concentration was performed in this study by quantitative PCR. In fact, culture-dependent methods can only detect the viable and culturable microbial agents, leaving out a significant portion of particulates of microbial origin including viable but non-culturable and dead microorganisms; furthermore, the majority of airborne particles of microbial origin, even when viable, is non-culturable and unable to form new colonies even appropriate media (Górny, 2020).
As expected, the amount of microbial load detected by molecular techniques was significantly higher compared to that found with methods culture-dependent, equal to 1 order of magnitude higher for fungi and 3 orders for bacteria.
Therefore, by combining molecular techniques with traditional and recognized microbiological techniques, it is possible to have a more complete picture of the microbial community present in the bioaerosol.

Physical characteristics of the aerosol inside the thermal cave

From the analysis of the data relating to the physical characteristics of the aerosol measured inside the thermal cave, it can be seen that the dimensional distribution in terms of number of particles results as tri-modal, with the first mode located around 0.3 µm, a second one around 3 µm and the last one around 8 µm, as showed in Fig. 1. It should be noted, anyway, that the two modes that mainly characterize the size distribution in terms of number are the first one (0.3 µm) and the last one (8 µm), while the mode at 3 µm results less pronounced. The size distributions in terms of surface area and mass of particles, on the contrary, resulted unimodal with mode at 10 µm (Fig. 1). From the analysis of the data, it can be stated that the dimensional distribution in number highlights the presence in the cave of a significant fraction of particles whose dimensions were below the detection threshold of the spectrometer (sub-micrometric particles) even if the fraction of particles with mode around 8 µm was predominant. On the other hand, both the distributions in terms of surface area and mass of particles were characterized with a mode totally shifted to higher particle diameters. Summarising, the analysis of the measured data indicated the presence in the cave of a significant fraction of sub-micrometric particles and a predominant fraction of super-micrometric particles contributing to the surface area and mass concentration. These super-micrometric particles consisted, presumably, of water droplets, while the sub-micrometric particles may consist of the solid nuclei, resulting from the evaporation of the volatile fraction, which remain suspended in air.

Risk of infection transmission inside the thermal cave

The analysis of the data reported in Table 6 allowed to characterize the cave in terms of risk of infection under the assumptions of the model and for the considered scenarios. First of all, considering the reported data, it should be highlighted the determining effect of the mechanical ventilation system on the risk of contagion: for all the hypothesized scenarios, there is a substantial reduction in the risk of contagion considering the ventilation system active (both for the individual susceptible subject in the 15 minutes of stay and for continuous occupation of the cave). This effect is made even more evident by the parameter relating to the maximum occupation of the cave (continuous occupation) which changes from the theoretical value of 75 to that of 605 (with ventilation system deactivated, S3, and activated, S1, respectively), and from 12 to 96 (with ventilation system deactivated, S4, and activated, S2, respectively). It should be highlighted, however, the purely theoretical role, albeit significant, of this parameter: it is unlikely, in fact, the simultaneous presence of more occupants than the surface of an indoor environment would allow.

Furthermore, from the analysis of the results, it is evident that the adoption of social distancing measures such as non-simultaneous access to the cave (S1) makes the risk of contagion extremely low, according to the assumptions of the model. even with the mechanical ventilation system not active. A condition that presents a relatively high risk for the single susceptible subject is that relating to the modelled scenario with the ventilation system not active and the presence of two infectious subjects and one susceptible subject at the same time in the cave talking to each other (S4). In this case, in fact, assuming a probability of infection of 0.1%, the maximum exposure time is less than the 15-minute of residence time for the susceptible subject (11 minutes). On the contrary, for scenario 1 with the ventilation system not active (S3), the maximum exposure time is less than the maximum time (54 minutes out of 480), highlighting, once again, the fundamental role of the mechanical ventilation system. Finally, from the analysis of Fig. 3, it can be seen that the mechanical ventilation system active results in a sudden reduction on the quanta concentration in the cave (solid lines in Fig. 3) that reaches a zero value after about 75 minutes for both S1 and S3 scenarios and in a consequent reduction of the risk of contagion (both individual risk, dashed lines, and continuous risk, dotted lines) and increase in maximum

occupancy (dashed-dotted lines). On the contrary, with the ventilation system not active, the quanta concentration reaches zero value after about 460 minutes for scenario 2 while for the worst hypothesized scenario (S4), the quanta concentration still remains greater than zero after the whole simulation period (480 minutes).
The authors want to highlight the main limitation of the model which lies in the "box model" approach, according to which the air is perfectly mixed in the cave and, consequently, the quanta concentration over time becomes uniform in space. According to this approach, susceptible individuals are therefore exposed to the same quanta concentration regardless of their position in the cave. Differences in exposure risk between susceptible occupants are therefore reduced to a function of the duration of exposure rather than their position in the cave. In the light of these simplifying hypotheses, the accuracy of the model depends on the spatial scale analysed. In general, the smaller the enclosed space, the more the air is mixed and therefore the closer the results are to reality.

Conclusions

The microbiological characterization of the bioaerosol inside the thermal cave highlighted a low microbial load, with a prevalence of non-cultivable strains generated by the aerosolization of the thermal waters. Although there are no worldwide accepted regulations for microbial air contamination, by comparing the data deriving from culture-dependent techniques with the indicative levels established by the European Collaborative Action (EUR 14988), the detected microbial load values can be classified as a very low level of contamination, therefore associated with a good air quality.
The physical characterization of the aerosol revealed a tri-modal dimensional distribution in terms of number of particles, with the first mode located around 0.3 µm, a second one around 3 µm and the last one around 8 µm. The size distributions in terms of surface area and mass of particles, on the contrary, resulted unimodal with mode at 10 µm. The analysis of the measured data indicated the presence in the cave of a significant fraction of sub-micrometric particles, whose main contribution lies in the number concentration, and a predominant fraction of super-micrometric particles contributing to the surface area and mass concentration. These super-micrometric particles consisted, presumably, of water droplets, while the sub-micrometric particles may consist of the solid nuclei, resulting from the evaporation of the volatile fraction, which remain suspended in air.
In terms of the risk of SARS-CoV-2 infection, evaluated under the hypotheses of the model, it is highlighted the decisive effect of the mechanical ventilation system on the risk of contagion: for all the hypothesized scenarios, there is a substantial reduction in the risk of contagion considering the ventilation system active. Furthermore, the adoption of social distancing measures such as non-simultaneous access to the cave makes the risk of contagion extremely low, according to the assumptions underlying the model, even with the mechanical ventilation system not active.

Declarations

Funding and acknowledgments

This work has been carried out within the framework of COVID-19 activities of I-SUM/CINTEST group and has received funding from both, University of Tuscia, Viterbo (Italy) under “Action for research activities related to COVID-19emergency” Rector note n°5445, 05-05-2020, and from Terme de Papi (Viterbo, Italy) within the study “Characterization of Bioaerosol in the Thermal Cave of Terme dei Papi and effect of environmental conditions in the decay and transmission of biological agents”

Competing interests

No competing interests to declare.

Availability of data and material

Data, models, or code generated or used during the study, that are not reported in the manuscript, are available from the corresponding author by request.

References

Altman, N. (2000). Healing springs: the ultimate guide to taking the waters. *Inner Traditions/Bear & Co.*

Buonanno, G., Morawska, L., & Stabile, L. (2020a). Quantitative assessment of the risk of airborne transmission of SARS-CoV-2 infection: prospective and retrospective applications. *medRxiv*, https://doi.org/10.1101/2020.06.01.20118984

Buonanno, G., Stabile, L., & Morawska, L. (2020b). "Estimation of airborne viral emission: Quanta emission rate of SARS-CoV-2 for infection risk assessment." *Environment International 141*.

Cabral, J. P. (2010). Can we use indoor fungi as bioindicators of indoor air quality? Historical perspectives and open questions. *Science of the total environment*, 408 (20), 4285-4295

Chatoutsidou, S.E., Lazaridis, M., (2019). Assessment of the Impact of Particulate Dry Deposition on Soiling of Indoor Cultural Heritage Objects Found in Churches and Museums/Libraries. J. Cult. Heritage 39, 221–228. https://doi.org/10.1016/j.culher.2019.02.017.

Chia, P. Y., Coleman, K. K., Tan, Y. K., Ong, S. W. X., Gum, M., Lau, S. K., & Son, T. T. (2020). Detection of air and surface contamination by SARS-CoV-2 in hospital rooms of infected patients. *Nature communications*, *11*(1), 1-7.

Crognale, S., Stazi, S. R., Firrincieli, A., Pesciaroli, L., Fedi, S., Petruccioli, M., & D'Annibale, A. (2019). Time-Dependent Changes in Morphostructural Properties and Relative Abundances of Contributors in Pleurotus ostreatus/Pseudomonas alcaliphila Mixed Biofilms, https://doi.org/10.3389/fmicb.2019.01819

European Collaborative Action Indoor Air Quality and its Impact on Man (formerly Cost Project 613) - Environment and Quality of Life. EUR 14988

Ghosh, B., Lal, H., & Srivastava, A. (2015). Review of bioaerosols in indoor environment with special reference to sampling, analysis and control mechanisms. *Environment international*, *85*, 254-272.

Górny, R. L. (2020). Microbial aerosols: sources, properties, health effects, exposure assessment—a review. *KONA Powder and Particle Journal*, 2020005.

Guo, Z. D., Wang, Z. Y., Zhang, S. F., Li, X., Li, L., Li, C., Zhang, M. Y. (2020). Aerosol and surface distribution of severe acute respiratory syndrome coronavirus 2 in hospital wards, Wuhan, China, 2020. *Emerg Infect Dis*, *26*(7), 10-3201.

International Commission on Radiological Protection (1994). Human respiratory tract model for radiological protection. A report of a Task Group of the International Commission on Radiological Protection, Annals of the ICRP. 24: 1-482.

Kohanski, M. A., Lo, L. J., & Waring, M. S. (2020). Review of indoor aerosol generation, transport, and control in the context of COVID-19. In *International forum of allergy & rhinology*, https://doi.org/10.1002/alr.22661

Li, Y., Qian, H., Hang, J., Chen, X., Hong, L., Liang, P., Kang, M. (2020). Evidence for probable aerosol transmission of SARS-CoV-2 in a poorly ventilated restaurant. *medRxiv*, https://doi.org/10.1101/2020.04.16.20067728

Liu, Y., Ning, Z., Chen, Y., Guo, M., Liu, Y., Gali, N. K., et al. (2020). Aerodynamic characteristics and RNA concentration of SARS-CoV-2 aerosol in Wuhan hospitals during COVID-19 outbreak. *BioRxiv*, https://doi.org/10.1101/2020.03.08.982637

Margarucci, L.M., Romano Spica, V., Gianfranceschi, G., Valeriani, F. (2019). Untouchability of natural spa waters: Perspectives for treatments within a personalized water safety plan. *Environment International*, 133, 105095.

Morawska, L., Tang, J. W., Bahnfleth, W., Bluyssen, P. M., Boerstra, A., Buonanno, G., Haworth, C. (2020). How can airborne transmission of COVID-19 indoors be minimised? *Environment international*, *142*, 105832.

Srikanth, P., Sudharsanam, S., & Steinberg, R. (2008). Bio-aerosols in indoor environment: composition, health effects and analysis. *Indian journal of medical microbiology*, *26*(4), 302.

Thomas, R. J., Webber, D., Sellors, W., Collinge, A., Frost, A., Stagg, A. J., et al. (2008). Characterization and deposition of respirable large-and small-particle bioaerosols. *Applied and environmental microbiology*, *74*(20), 6437-6443.

van Doremalen, N., Bushmaker, T., Morris, D.H., Holbrook, M.G., Gamble, A., Williamson, B.N., Tamin, A., Harcourt, J.L., Thornburg, N.J., Gerber, S.I., Lloyd- Smith, J.O., de Wit, E., Munster, V.J., (2020). Aerosol and Surface Stability of SARSCoV-2 as Compared with SARS-CoV-1. *N. Engl. J. Med.*

Workplace Atmosphere – Guidelines for Measurement of Airborne Micro-organisms and Endotoxin. EN 13098:2000.

Workplace atmosphere-Determination of airborne endotoxins. EN 14031:2003.

Workplace Atmospheres–Guide for the Application and Use of Procedures for the Assessment of Exposure to Chemical and Biological Agents. EN 14042: 2003.

Workplace atmospheres—volumetric bioaerosol sampling devices— requirements and test methods. EN 14583:2004.

World Health Organization (2020). Trasmission of SARS-CoV-2: implications for infection prevention precautions: scientific brief, 09 July 2020 (No. WHO/2019-nCoV/Sci_Brief/ Trasmission_modes/2020.3). World Health Organization

Figure Captions

Fig. 1 Particle size distributions of the aerosol measured inside the cave in terms of mass (M, in μg m^{-3}, solid line with circles), surface area (SA, in $μm^2$ cm^{-3}, dashed-dotted line with triangles) and number (N, in # cm^{-3}, dotted line with diamonds) of particles per volume unit of sampled air, in the range 0.3 µm to 10 µm in diameter, in 16 contiguous channels. Each dimensional channel value is reported as upper bound. The error bars represent the standard deviation in the measured data on each channel

Fig. 2 Deposition curves of particles, relative to the alveolar (ALV) and tracheobronchial (TB) regions of the respiratory system specific for adult women and men at rest (seated) who breathe mainly through the nose, a typical situation of the people who occupy the thermal cave

Fig. 3 Simulation results time course: scenario 1 (S1, ventilation system in operation, a); scenario 2 (S2, ventilation system not in operation, b); scenario 3 (S3, ventilation system in operation, c) and scenario 4 (S4, ventilation system not in operation, d). Quanta concentration (solid lines); continuous risk (dotted lines); individual infection risk (dashed lines) and maximum occupancy (dashed-dotted lines)

Fig.1

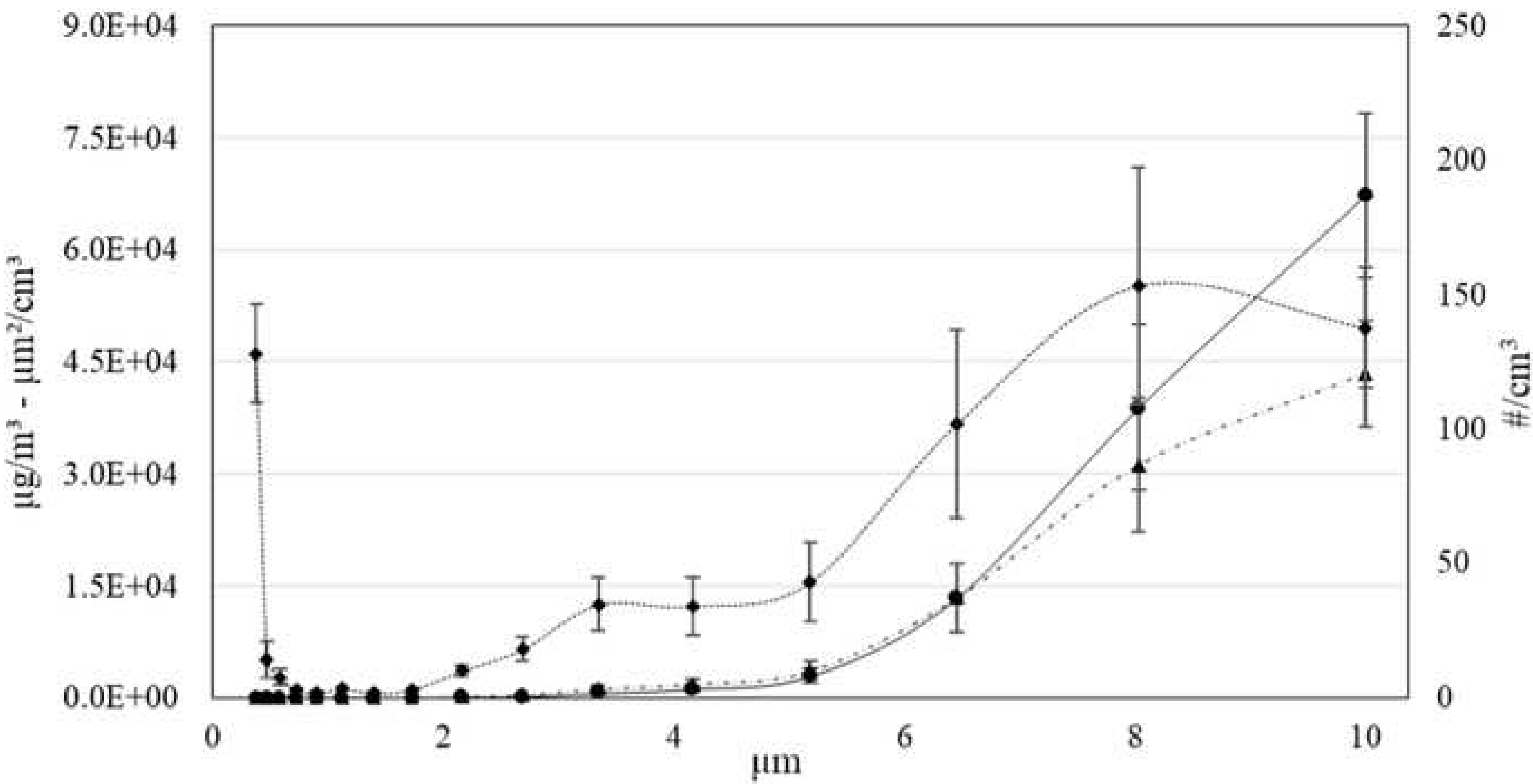
9.0E+04
7.5E+04
6.0E+04
4.5E+04
3.0E+04
1.5E+04
0.0E+00
μg/m³ - μm²/cm³
250
200
150
100
50
0
#/cm³
0
2
4
6
8
10
μm

Fig.2

Click here to access/download;Figure;Fig2.tiff

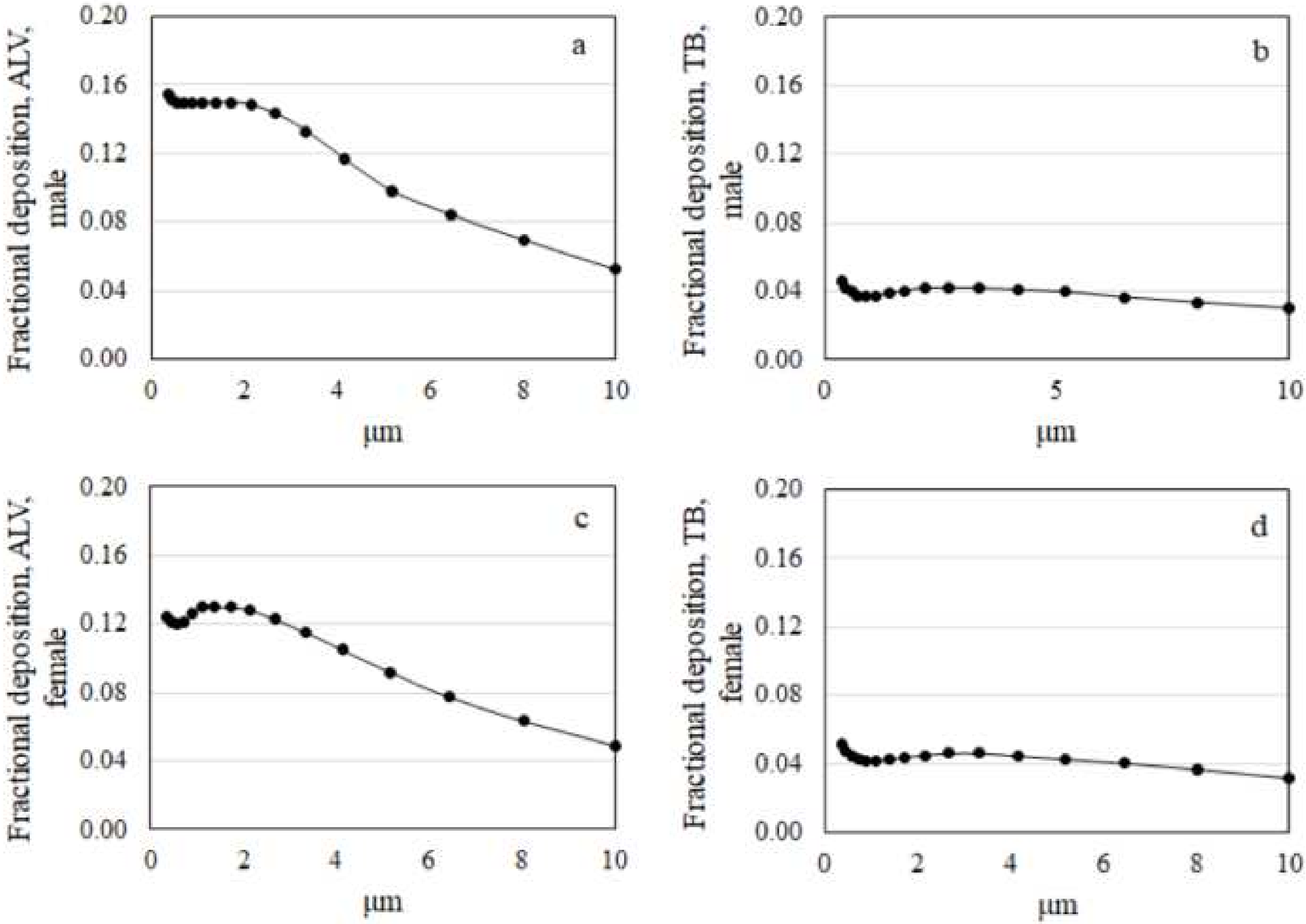

Fig.3

Click here to access/download;Figure;Fig3.tiff

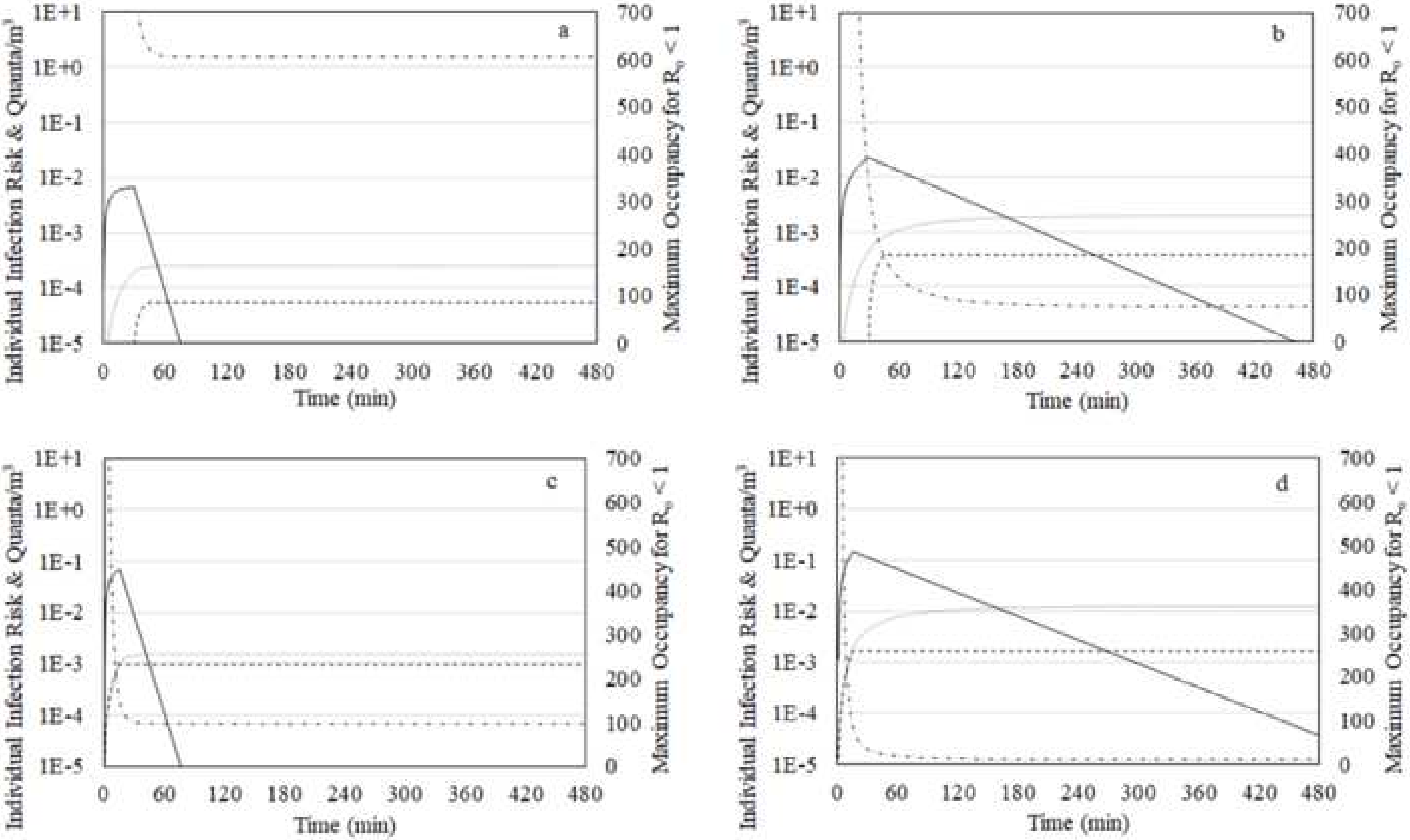

Table 1 Summary of the input data used in the model for calculating the risk of infection inside the thermal cave

V (m^3)	AER (h^{-1})	k (h^{-1})	λ (h^{-1})	n_0 (quanta/m^3)	t (minutes)
34	7.78	0.24	0.63	0	480

Table 2 Details of the exposure scenarios in the thermal cave implemented in the model (t_{in} = time of entry into the cave, t_{out} = time of exit from the cave, ER_q = emission rate of quanta, IR = inhalation rate, AER = air exchange rate)

Scenario	Infectious subject 1			Infectious subject 2			Susceptible subject			
	t_{in} (min)	t_{out} (min)	ER_q (quanta h^{-1})	t_{in} (min)	t_{out} (min)	ER_q (quanta h^{-1})	t_{in} (min)	t_{out} (min)	IR (m^3 h^{-1})	AER (h^{-1})
S1	0	15	2.0	15	30	2.0	30	45	0.49	7.78
S2	0	15	11.4	0	15	11.4	0	15	0.54	7.78
S3	0	15	2.0	15	30	2.0	30	45	0.49	0.2
S4	0	15	11.4	0	15	11.4	0	15	0.54	0.2

Table 3 Mean concentration of mesophilic and termophilic microbial load by means of active and passive sampling and of cultivation- independent techniques (nº gene copy /m^3)

	25°C	50°C	
Active sampling CFU/m^3	36±5^a	28±4^a	
Passive sampling CFU/(m^2·h)	3100±300^b	4330±240^a	
Cultivation independent techniques			
16S copy number/m^3	---	----	4.99E+04±8.84E+01
18S copy number/m^3	---	----	2.29E+02±3.54E-01

Different letters in apex indicate statistical significance according to Tukey's test, between values of microbial load obtained at 25 and 50 °C of incubation

Table 4 Average concentrations of the aerosol measured inside the cave in terms of number of particles per cm^3 of air (N), surface area of particles per cm^3 of air (SA) and mass of particles per m^3 of air (M)

	Average total concentration	Standard deviation
N (# cm^{-3})	6.9×10^2	1.3×10^2
SA (μm^2 cm^{-3})	9.5×10^4	2.2×10^4
M (μg m^{-3})	1.2×10^5	2.7×10^4

Table 5 Particle concentration in terms of number (N), surface area (SA) and mass (M) of particles deposited in the two regions of the respiratory system per unit of volume of inhaled air inside the cave (adults at rest, male - female, ALV = alveolar region, TB = tracheobronchial region)

	Male			**Female**		
	ALV	**TB**	**Total male**	**ALV**	**TB**	**Total female**
N (# cm^{-3})	68.02	25.84	93.86	59.46	28.37	87.83
SA (μm^{2} cm^{-3})	6.37×10^{3}	3.12×10^{3}	9.49×10^{3}	5.90×10^{3}	3.37×10^{3}	9.27×10^{3}
M (μg m^{-3})	7.85×10^{3}	4.00×10^{3}	1.18×10^{4}	7.30×10^{3}	4.29×10^{3}	1.16×10^{4}

Table 6 Simulation results for all the hypothesized scenarios referred to both the conditions of individual risk (susceptible subject) and continuous occupation of the thermal cave

	Susceptible subject					**Continuous occupation**					
Scenario	**t_{exp} (min)**	**R (%)**	**$t_{exp,0.1}$ (min)**	**$t_{exp,1}$ (min)**	**$O_{max,R0<1}$**	**t_{exp} (min)**	**R (%)**	**$t_{exp,0.1}$ (min)**	**$t_{exp,1}$ (min)**	**$O_{max,R0<1}$**	**AER (h^{-1})**
S1	15	0.01	>15	>15	2742	480	0.02	>480	>480	605	7.78
S2	15	0.1	>15	>15	156	480	0.15	15	>480	96	7.78
S3	15	0.04	>15	>15	386	480	0.20	54	>480	75	0.2
S4	15	0.16	11	>15	91	480	1.21	11	103	12	0.2